THE JOURNAL OF BIOLOGICAL CHEMISTRY VOL. 286, NO. 37, pp. 31975–31983, September 16, 2011

Apoptosis Induced by Persistent Single-strand Breaks in Mitochondrial Genome

*CRITICAL ROLE OF EXOG (5′-EXO/ENDONUCLEASE) IN THEIR REPAIR**[S]

Received for publication, December 22, 2010, and in revised form, July 8, 2011 Published, JBC Papers in Press, July 18, 2011, DOI 10.1074/jbc.M110.215715

Anne W. Tann[‡], Istvan Boldogh[§], Gregor Meiss[¶], Wei Qian[‖], Bennett Van Houten[‖], Sankar Mitra[‡], and Bartosz Szczesny[‡1]

From the Departments of [‡]Biochemistry and Molecular Biology and [§]Microbiology and Immunology, University of Texas Medical Branch, Galveston, Texas 77555-1079, the [¶]Institute of Biochemistry, Faculty of Biology and Chemistry, Justus-Liebig-University, Heinrich-Buff-Ring 58, 35392 Giessen, Germany, and the [‖]Department of Pharmacology and Chemical Biology, University of Pittsburgh Cancer Institute, Pittsburgh, Pennsylvania 15213-1863

Reactive oxygen species (ROS), continuously generated as by-products of respiration, inflict more damage on the mitochondrial (mt) than on the nuclear genome because of the nonchromatinized nature and proximity to the ROS source of the mitochondrial genome. Such damage, particularly single-strand breaks (SSBs) with 5′-blocking deoxyribose products generated directly or as repair intermediates for oxidized bases, is repaired via the base excision/SSB repair pathway in both nuclear and mt genomes. Here, we show that EXOG, a 5′-exo/endonuclease and unique to the mitochondria unlike FEN1 or DNA2, which, like EXOG, has been implicated in the removal of the 5′-blocking residue, is required for repairing endogenous SSBs in the mt genome. EXOG depletion induces persistent SSBs in the mtDNA, enhances ROS levels, and causes apoptosis in normal cells but not in mt genome-deficient rho0 cells. Thus, these data show for the first time that persistent SSBs in the mt genome alone could provide the initial trigger for apoptotic signaling in mammalian cells.

A mammalian cell contains up to several thousands copies of duplex, circular 16.5-kb mt[2] genome within 80–700 mitochondria depending on the cell type (1, 2). The mtDNA encodes essential subunits of the respiratory chain, tRNA and rRNAs, all of which are critical for maintaining oxidative phosphorylation (OXPHOS) (3). OXPHOS accounts for about 85% of oxygen consumed by the cell, and early reports estimated that under physiological conditions ~5% of consumed oxygen is partially reduced to ROS (4). Although recent reports indicate a much lower level of ROS production in normal cells, even a low and persistent ROS level has long term detrimental effects (5, 6). Thus, the mitochondria, the major cellular site for ROS generation, are under continuous oxidative stress that results in oxidative damage to DNA, as well as proteins and lipids (7).

ROS-induced DNA damage includes multitude of mutagenic oxidized bases and single-strand breaks (SSBs) containing 3′- and 5′-blocking groups in DNA, which are generated both directly or as intermediates during BER (8, 9). Because of close proximity of the site of ROS generation and nonchromatinized state of the mt genome, the mutation rate in human mtDNA is 20–100-fold higher relative to the nDNA (10). As summarized in recent reviews (11–13), repair of oxidized base lesions or abnormal bases is initiated with their excision by a DNA glycosylase. A monofunctional glycosylase, such as uracil-DNA glycosylase, excises U from the DNA to generate an abasic (AP) site, which is then cleaved by AP endonuclease (APE1) in mammalian cells to generate 3′-OH and nonligatable 5′-deoxyribose phosphate (dRP) residues. In the nucleus, the 5′-dRP could be removed by DNA polymerase β (pol β) via its intrinsic dRP lyase activity. In the mitochondria, the DNA polymerase γ (pol γ) with similar dRP lyase activity is also able to remove the dRP moiety (14). In the case of oxidized base repair by DNA glycosylases with intrinsic AP lyase activity, such as 8-oxoguanine-DNA glycosylase (OGG1), base excision is coupled to strand cleavage at the AP site with generation of 5′-phosphate and 3′-blocking phospho-α,β-unsaturated aldehyde that is subsequently removed by the intrinsic 3′-phosphodiesterase activity of APE1. This leaves a 3′-OH that serves as the primer terminus for DNA repair synthesis. However, the absence of an aldehyde group in oxidized deoxyribose fragment at the 5′ terminus after the DNA strand break, as in the case of oxidized AP sites, precludes their removal by the dRP lyase activity of pol β and γ in the nucleus and mitochondria, respectively. In such a case, the 5′-blocking group in nDNA together with additional nucleotides are removed by flap endonuclease 1 (FEN1), a 5′-exo/endonuclease. Thus, the resulting gap filling by a DNA polymerase and nick sealing by DNA ligase during BER could proceed via two subpathways as follows: single nucleotide-BER, where only the damage base is replaced, or long patch (LP)-BER, where 2–6 additional nucleotides at the 5′ terminus are removed by a 5′-exo/endonuclease followed by resynthesis. In the nucleus, DNA ligase3 (lig3) is involved in single nucleotide-

* This work was supported, in whole or in part, by National Institutes of Health Grants P01 AG10514 and R01 CA53791 (to S. M.) and P01 AG021830 (to I. B.) from USPHS and Training Grants T32 ES07254 and 5F30 ES017207-02 (to A. W. T.). This work was also supported by Pennsylvania CURE (to B. V. H.) and the Dr.-Herbert-Stolzenberg-Stiftung of the Justus-Liebig-University Giessen (to G. M.).

[S] The on-line version of this article (available at http://www.jbc.org) contains supplemental "Experimental Procedures" and Figs. S1–S8.

[1] To whom correspondence should be addressed. Tel.: 409-772-2174; Fax: 409-747-8608; E-mail: baszczes@utmb.edu.

[2] The abbreviations used are: mt, mitochondrial; ROS, reactive oxygen species; SSB, single-strand break; SSBR, SSB repair; BER, base excision repair; OXPHOS, oxidative phosphorylation; OCR, oxygen consumption rate; nt, nucleotide; pol, polymerase; EndoG, endonuclease G; dRP, 5′-deoxyribose phosphate; h, human; 7-AAD, 7-amino-actinomycin D; THF, tetrahydrofuran.

BER after pol β fills in the single nucleotide gap. FEN1-mediated gap is likely to be filled in by replicative DNA polymerases δ/ε followed by nick sealing with DNA ligase1 (lig1), although pol β has also been implicated (15). In contrast to the situation in the nucleus with multiple DNA polymerases and ligases, their sole mt counterparts, pol γ and lig3, are responsible for both replication and repair of mtDNA (16).

Only single nucleotide-BER activity was known in the mitochondria until we and others discovered LP-BER activity in mt extract of mammalian cells; however, the identity of the mt 5′ end-processing exo/endonuclease was not settled (17–20). Our group and Akbari *et al.* (20) reported that mt LP-BER is FEN1-independent. We detected the presence of an unknown 5′-exo/endonuclease activity in mt extract of mammalian cells that generated short (2–4 nucleotides) fragments, distinct from those generated by FEN1 (18). In contrast, Liu *et al.* (19) have shown that repair of 2-deoxyribonolactone, a common AP site oxidation product, was dependent on FEN1 activity. Subsequently DNA2, a helicase/nuclease, which plays various roles in the processing of nDNA intermediates during replication and repair in yeast, was shown to be present in the human mitochondria and was proposed to process 5′-flap intermediates in DNA, synergistically with FEN1 during mtDNA replication and LP-BER (21). In addition, another 5′-exo/endonuclease, EXOG, which localized exclusively in mitochondria, was identified as a paralog of endonuclease G (EndoG), with nuclease activity toward single-strand DNA; however, its role in the maintenance of mt genome was not determined (22).

In this study, we investigated the role of the three mt 5′-exo/endonucleases and have shown that EXOG but not FEN1 nor DNA2 provides the critical 5′-exonuclease activity for mt BER/SSBR. EXOG depletion causing accumulation of persistent SSBs in the mt, but not in nu genome, increases oxidative stress and induces mt dysfunction, thereby activating the intrinsic apoptotic pathway. More importantly, we have shown for a first time that persistent SSBs in the mt genome alone trigger apoptosis in mammalian cells, which is suppressed in cells deficient in mtDNA. Those results underscore the importance of mt genome integrity in cell survival.

EXPERIMENTAL PROCEDURES

Cell Culture—The human lines HeLa, MCF7, and HCT 116 ($p53^{+/+}$) were grown in DMEM and McCoy's media, respectively. A549 cells were grown in F-12 medium. Respiration-deficient (A549 rho0) cells were established by maintaining A549 cells in the culture medium containing 50 ng/ml ethidium bromide for >60 population doublings. When cells became respiration-deficient, the medium was supplemented with 50 μg/ml uridine, 120 μg/ml sodium pyruvate, and 50 ng/ml ethidium bromide (23). All cell lines were obtained from the American Type Culture Collection (ATCC). The culture media were supplemented with 50 units/ml penicillin, 50 μg/ml streptomycin and 10% heat-inactivated FBS.

Preparation of Whole Cell, Nuclear and Mitochondrial Extract, Western Blot, and Immunoprecipitation—Whole cell, nuclear and mitochondrial extracts were prepared as described earlier (24). Protein concentrations were determined using Bradford reagent (Bio-Rad) and using bovine serum albumin (BSA) as the standard. Western analysis was performed as described previously (25) using the following antibodies: EXOG (Sigma), GAPDH (Cell Signaling), FEN1 (Bethyl Laboratories or GeneTex, Inc.), DNA pol γ (Abcam), DNA Lig3 (QED Bioscience Inc.), poly(ADP-ribose) polymerase (Santa Cruz Biotechnology), caspase-9, caspase-8, and caspase-3 (Cell Signaling), 56-kDa subunit of mt complex V, and ND-37 37-kDa subunit of mt complex I (Invitrogen). FLAG-peptide immunoprecipitation was performed as described earlier (18) using FLAG M2-agarose beads incubated with ~1 mg of mitochondrial extract isolated from HeLa cells transiently transfected with human EXOG containing FLAG on the C terminus. Human EXOG cDNA was cloned into p3×-FLAG-CMV-14 vector (Sigma) as described previously (22).

Protein Depletion with siRNA—HeLa, HCT 116, or A549 cells were transfected with 40 nM siRNA specific for FEN1 (Santa Cruz Biotechnology, catalog no. sc-37795), DNA2 (Santa Cruz Biotechnology, catalog no. sc-90458), EXOG (Invitrogen, catalog no. ENDOGL1HSS115057), or control using Lipofectamine 2000 (Invitrogen) per the manufacturer's protocol. To optimize the siRNA concentration for maximal target depletion, preliminary transfections were carried out with 10–100 nM for each siRNA. The level of depletion was calculated by densitometric analysis of Western blots relative to loading control of three independent experiments using Gel Logic 2200 and Molecular Imaging software (Kodak).

RT-PCR—The mRNA depletion of individual nucleases was evaluated by RT-PCR using OneStep RT-PCR kit (Qiagen) per the manufacturer's recommendations, and the following pairs of primers were used: EXOG 5′-TTT TCT GAG CGG CTT CG T-3′ (sense) and 5′-TGA TCT TTT CCA GTC TGA GCA-3 (antisense); FEN1 5′-CCT GGC CAA ACT AAT TGC TGA-3′ (sense) and 5′-TCC CCT TTT AAA CTT CCC TG-3 (antisense); DNA2 5′-TCC GCT CTG CTG TTG ACA ATA-3′ (sense) and 5′-TCA GTT TAT GTT TGG CTC TGG-3 (antisense). Preliminary assays were carried out to ensure the linearity of PCR amplification with respect to number of cycles and RNA concentration.

Assessment of Apoptosis, Superoxide Anion Level, and Mitochondrial Membrane Depolarization—Early apoptotic, late apoptotic, and necrotic populations were characterized using the annexin V-PE apoptosis detection kit (Pharmingen) per the manufacturer's protocol. MitoSOX Red (Molecular Probes) was used to assess the level of superoxide anion generated in the mitochondria, according to the manufacturer's recommendations. Mt membrane depolarization was analyzed using the MitoProbe JC-1 assay kit (Molecular Probes). In all cases, the cells were analyzed by flow cytometry (FACSCanto (BD Biosciences) at the University of Texas Medical Branch Flow Cytometry and Cell Sorting Core).

Extracellular Flux Analysis—Oxygen consumption rate (OCR) and extracellular acidification rate were measured using a Seahorse XF24 Extracellular Flux Analyzer (Seahorse Bioscience, North Billerica, MA) as described previously (26). Briefly, on the day before extracellular flux analysis, siRNA-transfected MCF7 cells were trypsinized and subcultured in an XF24 cell culture plate at 4×10^4 cells/well and incubated in 5% CO_2 incubator at 37 °C for overnight. The cells were then washed,

and the growth medium was replaced with unbuffered DMEM. After incubating cells for another 60 min in a 37 °C incubator without CO_2, the OCR and extracellular acidification rate measurements were performed simultaneously.

Quantification of DNA Damage—Gene-specific semi-quantitative PCR assays for measuring DNA damage were performed as described earlier (27) using LongAmp TaqDNA polymerase (New England Biolabs). Preliminary assays were carried out to ensure the linearity of PCR amplification with respect to the number of cycles and DNA concentration. Damage to mtDNA was normalized to mt genome copy number determined by amplification of a 211-bp fragment.

DNA Repair Synthesis Assay—The DNA repair assay was carried out as described earlier (18, 28). Briefly, the 20-μl assay mixture contained 20 μM each of four unlabeled dNTPs, 4 μCi of [α-^{32}P]dATP, mitochondrial or nuclear protein extract (5–10 μg), and duplex oligonucleotide substrate in assay buffer. After incubation at 37 °C for 30 min, the products were separated from the substrates by electrophoresis in a 20% acrylamide, 7 M urea gel. The radioactivity in these bands was quantitated in a PhosphorImager (GE Healthcare) using ImageQuant software. Preliminary enzyme assays were carried out to ensure the linearity of the reaction with respect to both time and the amount of extract. To rule out strand displacement during LP-BER, we also performed repair assay using 3′-^{32}P-labeled oligonucleotide (18). The specific activity of AP endonuclease was calculated as reported previously (29). Recombinant EXOG was purified, and its specific activity was determined using gap- and flap-specific substrates as described earlier (18, 30).

Statistical Analysis—At least three independent experiments were carried out in duplicate or triplicate for each assay. The results are presented as means ± S.E. and analyzed for statistical significance with one-way analysis of variance.

RESULTS

EXOG Depletion Triggers Cell Death—To evaluate the role of mt 5′-exo/endonucleases, we used appropriate siRNAs to individually knock down EXOG, FEN1, and DNA2 to 10–20% of their endogenous levels at 48 h post-transfection in HeLa and HCT 116 (p53$^{+/+}$) cells. The reduction in enzyme and mRNA levels was calculated by semi-quantitative RT-PCR and densitometric analysis of Western blots (Fig. 1, *A* and *B*). Massive cell death was observed only after depleting EXOG, but not FEN1 nor DNA2, as assessed by plasma membrane permeability and externalization of phosphatidylserine. Such analysis discriminates early apoptotic (annexin V-positive, 7-amino-actinomycin D (7-AAD)-negative) from late apoptotic (annexin V-positive, 7-AAD-positive) or necrotic (annexin V-negative, 7-AAD-positive) cell populations (31, 32). We observed a significant increase in the levels of early and late apoptotic but not necrotic cell populations at 48 h post-transfection in EXOG-depleted cells for both lines, but not after depleting FEN1 nor DNA2 (Fig. 1, *C* and *D*, and supplemental Fig. 1, *A* and *B*). Only prolonged (4-day) incubation with FEN1-siRNA caused apoptosis (data not shown), presumably due to the essential role of FEN1 in maintaining integrity of the nu genome and thus cell survival (19). However, we did not detect any type of cell death after DNA2 depletion, even after longer (4-day) siRNA treatment (data not shown). Although mtDNA replication is independent of the cell cycle (33), we tested the effect of depletion of each of the three 5′-exo/endonucleases on the level of BrdU incorporation into DNA of HCT cells stained with 7-AAD at 48 h after siRNA transfection (34). Significant increase (~5-fold) in the sub-G_1 cell population was observed only after depletion of EXOG compared with the control (supplemental Fig. 2, *A* and *B*), which further supports our conclusion that EXOG depletion activates cell death.

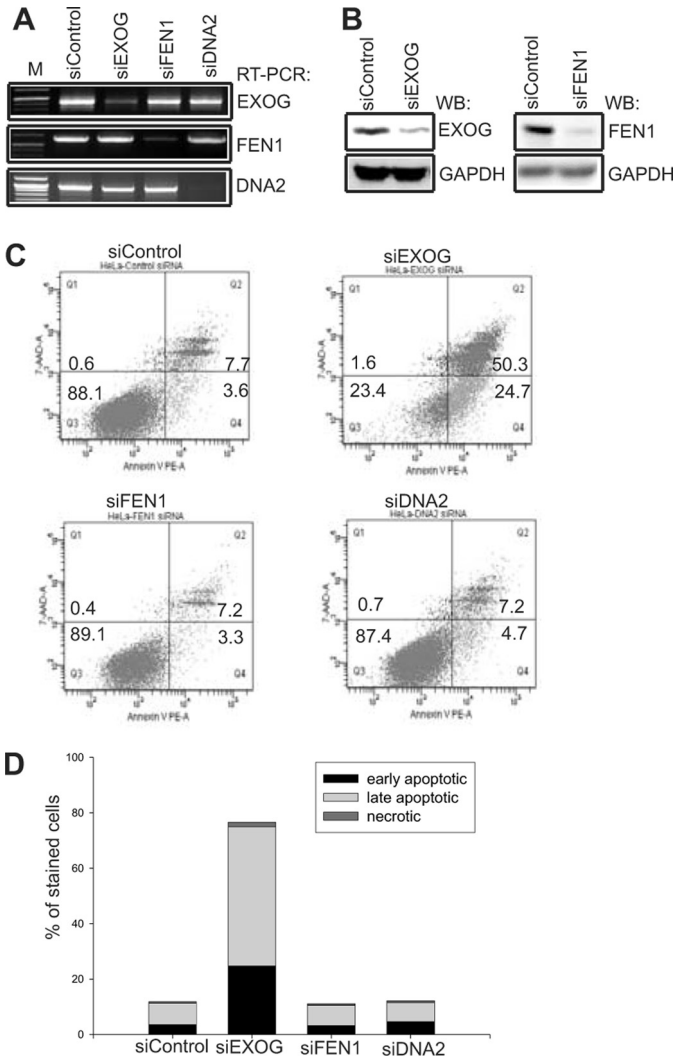

FIGURE 1. **Effects of mt 5′-exo/endonuclease depletion on cell viability.** *A*, mRNA levels of EXOG, FEN1, and DNA2 as measured by semi-quantitative RT-PCR. *Lane M*, marker lane. *B*, Western blot (*WB*) analysis for EXOG and FEN1 in HeLa cells at 48 h after transfection. The DNA2 polypeptide was not analyzed due to lack of high quality commercial antibodies. *C*, viability of HeLa cells after transfection with individual siRNAs was measured by staining with annexin V and 7-AAD, followed by flow cytometry. *D*, quantification of early apoptotic, late apoptotic, and necrotic populations in EXOG-, FEN1-, and DNA2-depleted HeLa cells. The mean result of three independent experiments is shown.

Depletion of EXOG Activates Intrinsic Apoptotic Pathway Because of Mitochondrial Dysfunction—Apoptosis typically occurs via the intrinsic or extrinsic pathways, which in turn activate the executioner caspases, caspase-3 and caspase-7, respectively (35). Intrinsic apoptotic pathway usually involves loss of mt transmembrane potential and change in ROS gener-

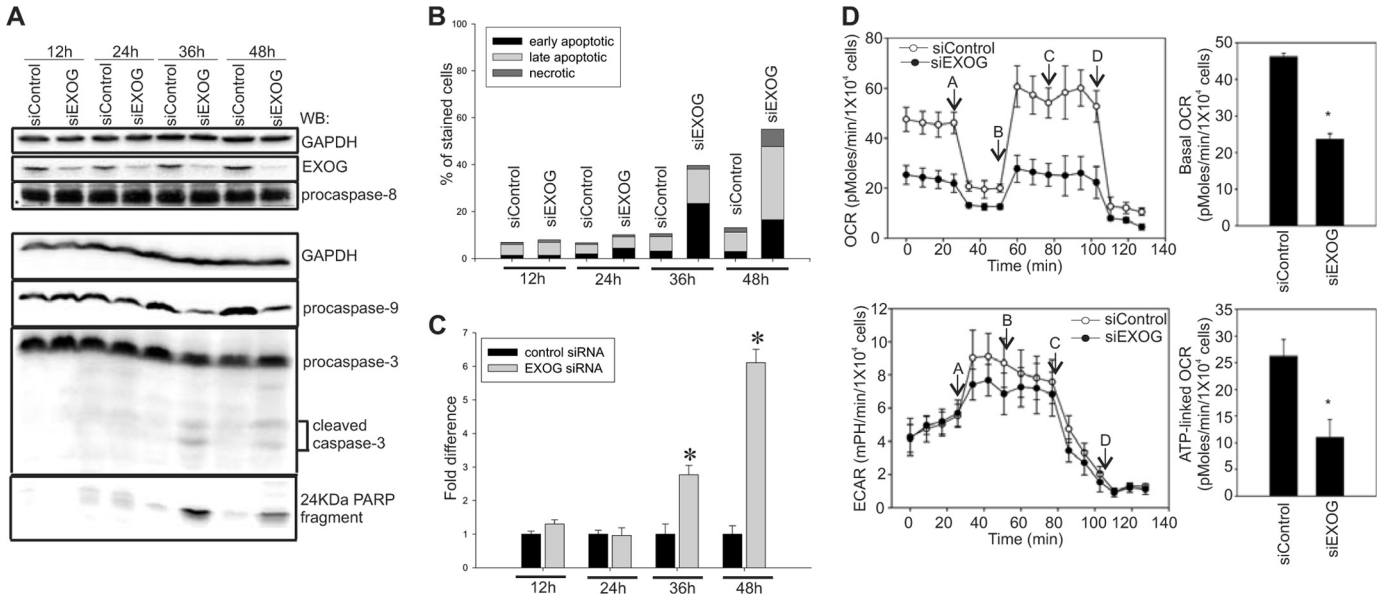

FIGURE 2. **EXOG depletion induces mitochondrial dysfunction and programmed cell death.** *A,* Western blot (*WB*) analysis of EXOG depletion and caspase activation at various times after transfection of HeLa cells with EXOG-siRNA compared with control siRNA. GAPDH was used as a loading control. Proteins separated on 12.5% SDS-PAGE were probed with antibodies as indicated. *B,* quantitation of early apoptotic, late apoptotic, and necrotic cell populations in HeLa cells at 12, 24, 36, and 48 h post-transfection with EXOG siRNA. The mean result of three independent experiments is shown. *C,* level of superoxide anion was measured by MitoSOX Red staining in EXOG siRNA-transfected HeLa cells compared with control. The mean results ± S.E. of three independent experiments is shown. * indicates $p < 0.05$ compared with control. *D,* OCR and extracellular acidification rate (*ECAR*) were measured 48 h after EXOG-siRNA transfection of MCF7 cells as described under "Experimental Procedures." The inhibitors were injected sequentially at indicated time points as follows: *A,* oligomycin (1 μg/ml); *B,* carbonyl cyanide *p*-trifluoromethoxyphenylhydrazone (0.3 μM); *C,* 2-deoxyglucose (100 mM); *D,* rotenone (1 μM). The data are representative of two independent experiments performed in replicates of five. Basal OCR is the mean of first four time points prior to injection A. ATP-linked OCR is the basal OCR (mean of points 1–4) minus the oligomycin level of OCR (mean of points 5–7). Student's *t* test was used to compare mean values, $p < 0.001$.

ation (36, 37). We tested how EXOG deficiency activated the apoptotic pathway at various times after siRNA transfection of HeLa cells. The EXOG level was reduced by 50% at 12 h after siRNA transfection and by 80–90% after 36–48 h (Fig. 2*A*). This was accompanied by a significant decrease in the procaspase-9 level at 36 and 48 h post-transfection, together with activation of caspase-3 but not of caspase-8 (Fig. 2*A*). In addition, the 24-kDa poly(ADP-ribose) polymerase cleavage product, an apoptosis hallmark (38, 39), was detected at 36 and 48 h after EXOG depletion (Fig. 2*A*). Increase in early apoptotic cells could be observed at 24 h after EXOG-siRNA transfection and late apoptosis at 36 h (Fig. 2*B*). The lack of an off-target effect in activation of caspase-3 was tested by co-expression siRNA-resistant EXOG, which prevented caspase-3 activation (data not shown). Depolarization of the mt membrane potential significantly increased at 36 and 48 h after transfection compared with control after depletion of EXOG but not of FEN1 nor DNA2 (supplemental Fig. 3, *B–D*). Moreover, superoxide generation, presumably due to the loss of mt membrane potential (40), was observed only in EXOG-depleted cells but not FEN1- nor DNA2-depleted cells (Fig. 2*C* and supplemental Fig. 4, *A* and *B*). These results indicate that EXOG depletion causes a loss of mt functions, which in turn activates the intrinsic apoptotic pathway.

To test whether EXOG depletion affects mt function, we knocked down EXOG in MCF7 cells and studied oxygen consumption using a Seahorse Flux analyzer. This instrument simultaneously measures the OCR, a measure of OXPHOS, and extracellular acidification rate, a measure of lactate production via glycolysis (26). MCF7 breast cancer cells were chosen for these experiments because of their caspase-3 deficiency (41, 42) and therefore would be expected not to undergo apoptosis following loss of EXOG. Apoptosis could alter oxidative phosphorylation and might obscure any direct effects of EXOG depletion. EXOG knockdown in MCF7 cells reduced basal OCR and ATP-linked OCR by over 2-fold (Fig. 2*D* and supplemental Fig. 5). Surprisingly, these cells did not show compensatory increase in glycolysis. These data indicate that loss of EXOG causes a decline in OXPHOS capacity and therefore overall bioenergetics in the cell.

EXOG Depletion Decreases Mitochondrial Genome Integrity—To evaluate the contribution of EXOG, FEN1, and DNA2 to the maintenance of mt genomic integrity, we measured the level of damage in mt and nDNA by semi-quantitative PCR of long genomic fragments (27). This assay measures the integrity of both mt and nu genome, by quantifying mostly SSBs because the majority of oxidatively damaged base lesions in the genomes are by-passed by DNA polymerases (8, 43). The mitochondrion-specific DNA fragment in EXOG-depleted HeLa cells had 25 and 50% less amplification relative to the control at 24 and 48 h after siRNA transfection, respectively (Fig. 3*A* and supplemental Fig. 6*A*). In contrast, 20% less amplification was observed for a nucleus-specific DNA region in EXOG-depleted cells only at 48 h after siRNA transfection (Fig. 3*B* and supplemental Fig. 6*A*). The level of nDNA damage was further investigated by Comet analysis in alkaline condition of HeLa cell DNA (44), which showed no significant increase in the tail moment at 48 h after EXOG-siRNA transfection (supplemental Fig. S7). These results indicate that EXOG depletion causes accumulation of SSBs predominantly in the mt genome. How-

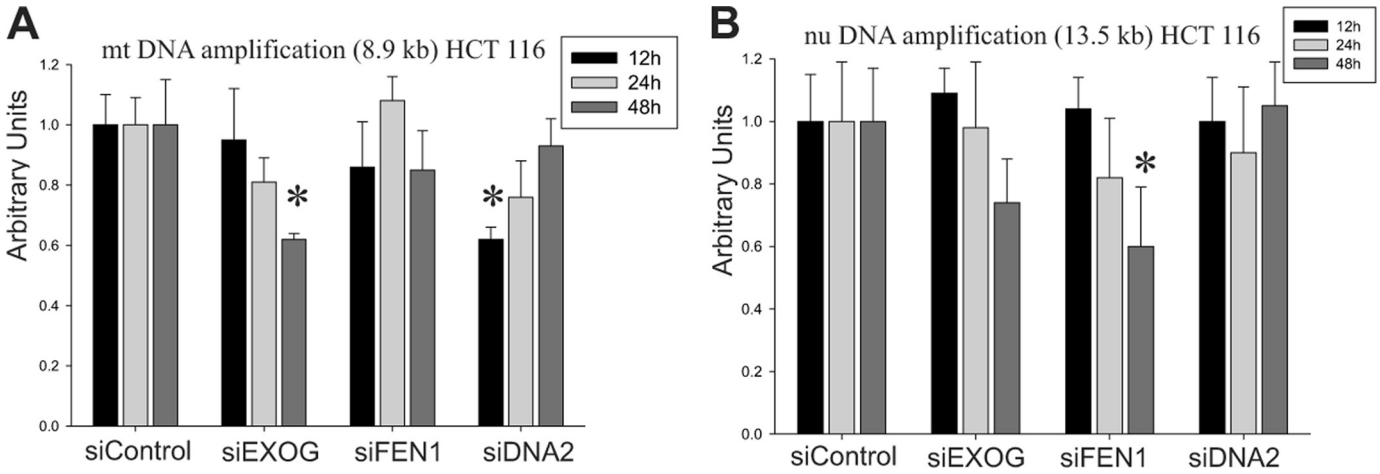

FIGURE 3. **Accumulation of DNA damage in the mt and the nu genomes after depletion of mt 5′-exonucleases in HeLa cells.** Quantitation of amplified mt and nDNA fragments for all three nucleases is shown in *A* and *B*, respectively. Damage to mt genome was normalized according to mt genome copy number. The mean results ± S.E. of three independent experiments are shown. * indicates $p < 0.05$ compared with control.

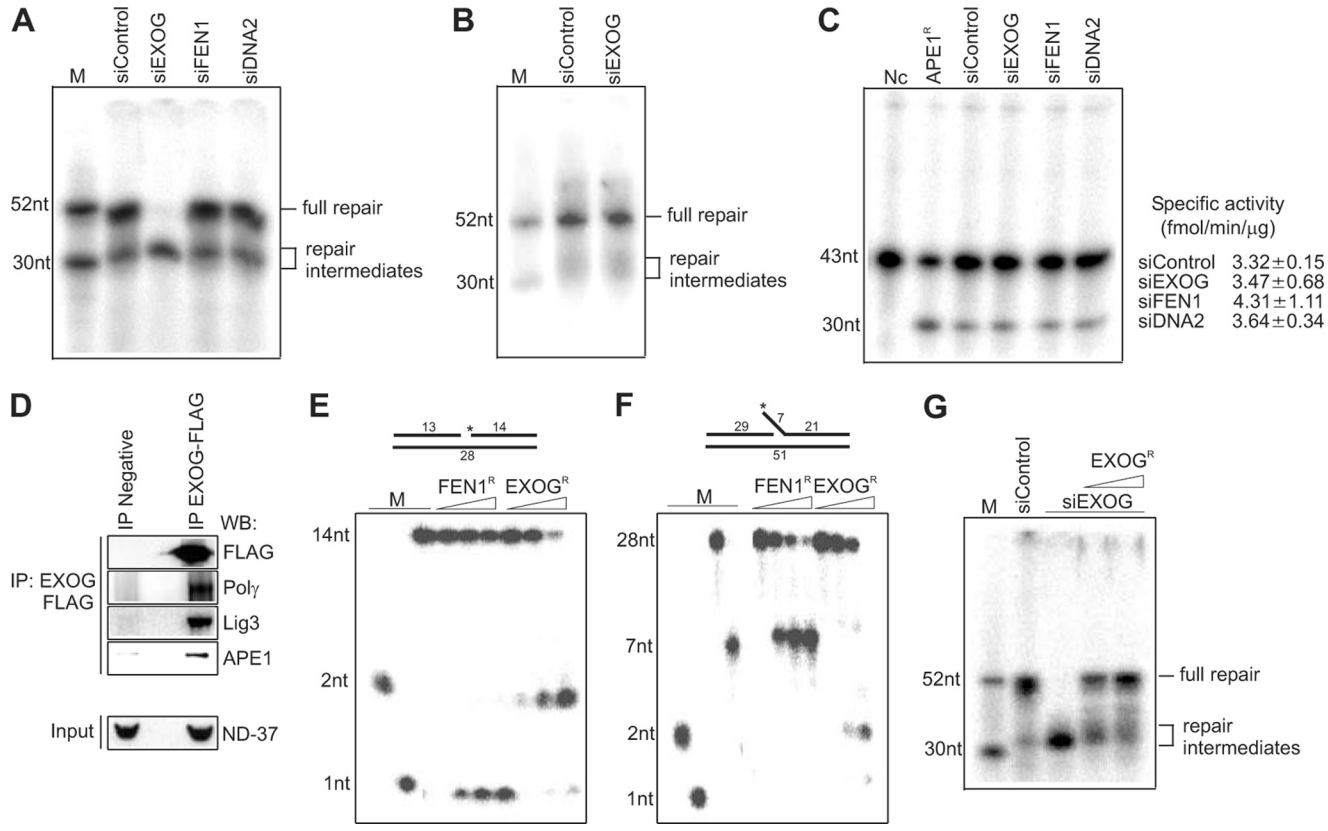

FIGURE 4. **EXOG provides critical 5′-exonuclease activity for Mt LP-BER.** DNA repair synthesis assays with mt (*A*) and nu (*B*) extract of HeLa cells after depletion of EXOG, FEN1, or DNA2 and 52-nt THF-containing oligonucleotide duplex. *C*, APE1 endonuclease activity was measured using ^{32}P-5′-label 43-nt-long THF oligonucleotide. The specific activity of APE1 in mt extract of EXOG-, FEN1-, or DNA2-depleted cells of three independent experiments is shown. *Nc*, represents control reaction without extract. APE1^{R}, reaction with recombinant APE1 protein. *D*, EXOG-FLAG immunocomplex isolated from HeLa cells contained mt DNA pol γ, DNA Lig3, and APE1. The 37-kDa subunit of NADH dehydrogenase (*ND-37*) was used as an input control. Specific EXOG activity with gap (*E*) and flap (*F*) DNA substrates were analyzed in comparison with FEN1. Increasing amounts of recombinant proteins were used (100, 200, and 400 fmol). *G*, DNA repair activity in mt extract of HeLa cells transfected with control or EXOG-specific siRNA using 52-nt THF oligonucleotide duplex substrate. 100 or 200 fmol of recombinant EXOG was added to assay mixture as indicated. The substrate and product were separated with 20% acrylamide, 8 M urea gels (for *A, B, C, E, F,* and *G*). *Lane M*, ^{32}P-5′-labeled marker oligonucleotides.

ever, FEN1 depletion did not affect the integrity of the mt genome under similar conditions, although accumulation of nDNA damage was observed (Fig. 3, *A* and *B*, and supplemental Fig. 6*B*). We conclude that the primary role of FEN1 is to maintain integrity of the nu genome, as was also suggested earlier (18, 20, 45). Interestingly, DNA2 depletion had no sustained effect on the integrity of the nu genome, although an early increase in mtDNA damage was detected (at 12 h post-transfection), which appears to have been subsequently repaired (Fig. 3, *A* and *B*, and supplemental Fig. 6*C*). These results sug-

gest that DNA2 is also involved in maintaining mt genome integrity, but its deficiency is eventually compensated by EXOG or other yet unknown 5′-exonuclease(s) as suggested earlier (21).

EXOG Provides Critical 5′ End Processing Activity for Mitochondrial LP-BER/SSBR—The repair of SSBs containing 5′-blocking oxidized deoxyribose fragments in mtDNA would require 5′ end-processing by one of the 5′-exo/endonucleases, which our results so far indicate to be EXOG. To confirm that EXOG contributes most if not all of the 5′ end-processing activity, we examined repair activity of mt extract for the AP analog tetrahydrofuran (THF) incorporated in a duplex oligonucleotide (18). THF is an AP site mimic whose repair is initiated by APE1 to generate 3′-OH and 5′-THF phosphate; the latter is resistant to 5′-AP lyase activity of pol γ. Thus, its removal prior to ligation of strand break would require a 5′-exonuclease. A 52-nt band signifying complete repair was observed with mt extract from control, FEN1-, or DNA2-depleted cells (Fig. 4*A*). However, a 32–34-nt band, corresponding to the repair intermediate product prior to repair synthesis, was generated with the mt extract from EXOG-depleted cells (Fig. 4*A*). This indicates that EXOG provides the critical 5′ end-cleaning activity that could not be substituted with FEN1 or DNA2. Thus, EXOG deficiency would generate SSBs as incomplete repair products in the mt genome as we have documented earlier. Furthermore, this observation indicates the lack of strand displacement in our assay that does not require 5′ end-processing. We performed similar *in vitro* DNA repair synthesis assays with nu extract from control and EXOG-depleted cells and did not observe any significant difference, which further confirms the role of EXOG as the 5′ end-cleaning enzyme specifically for mt SSBR (Fig. 4*B*). In addition, we observed similar levels of AP endonuclease activity, the primary 3′ end-cleaning enzyme in mammalian cells in mt extract from cells in which 5′-exo/endonucleases were individually depleted (Fig. 4*C*). Based on our previous observation that mt repair proteins form a complex for performing BER/SSBR (18), we isolated EXOG immunocomplexes from mt extract and demonstrated the presence of APE1, DNA lig3, and the catalytic subunit of DNA pol γ (Fig. 4*D*). Because our previous report indicated the presence of an unknown 5′-exonuclease generating short DNA products with gap or flap DNA substrates (18), we tested EXOG-specific activity using similar gap and flap DNA substrates. Regardless of the substrate type, we consistently observed a 2-nt reaction products (Fig. 4, *E* and *F*). In addition, we performed DNA repair synthesis assay with mt extract isolated from HeLa cells transfected with control or EXOG-specific siRNA and showed that the loss of full-length repair product with EXOG-depleted extract could be restored when recombinant EXOG protein was added to the reaction mixture (Fig. 4*G*). These results clearly established EXOG as the major 5′-exonuclease for mt LP-BER.

Mitochondrial DNA-depleted Cells Are Resistant to Cell Death Because of EXOG Deficiency—Our studies so far indicate that the accumulation of unrepaired SSBs generated in mtDNA induces the intrinsic apoptotic pathway. To test this further, we utilized A549 cells in which the mtDNA was depleted to an undetectable level (rho0) prior to EXOG knockdown (Fig. 5*A*). siRNA transfection resulted in >80% reduction of EXOG poly-

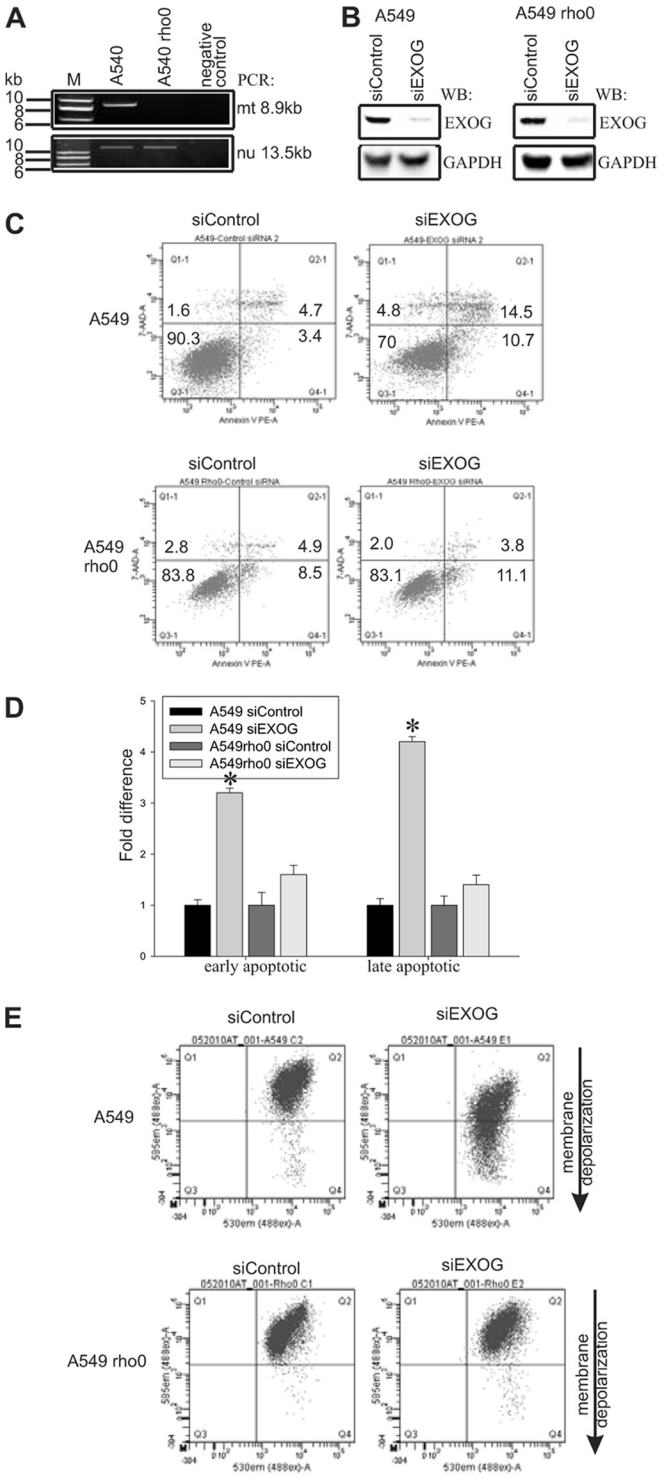

FIGURE 5. **Mt genome-deficient cells are resistant to cell death due to EXOG deficiency.** *A,* level of mtDNA in A549 rho0 cells was assayed by PCR amplification of long nucleus- and mitochondrion-specific DNA fragments indicating undetectable levels of mtDNA in A549 rho0 cells. *B,* Western blot (*WB*) analysis showing the level of EXOG depletion in A549 and A549 rho0 cells. *C,* viability of A549 and A549 rho0 cells after EXOG depletion was measured by staining with annexin V and 7-AAD at 48 h after siRNA transfection. *D,* quantitation of early apoptotic and late apoptotic cells in EXOG-depleted A549 and A549 rho0 cells at 48 h after siRNA transfection (shown as fold differences). The mean results ± S.E. of three independent experiments is shown. * indicates $p < 0.05$ compared with control. *E,* analysis of the mt membrane potential in EXOG-depleted A549 (*upper panel*) and A549 rho0 (*lower panel*) compared with control cells 48 h after siRNA transfection measured by flow cytometry.

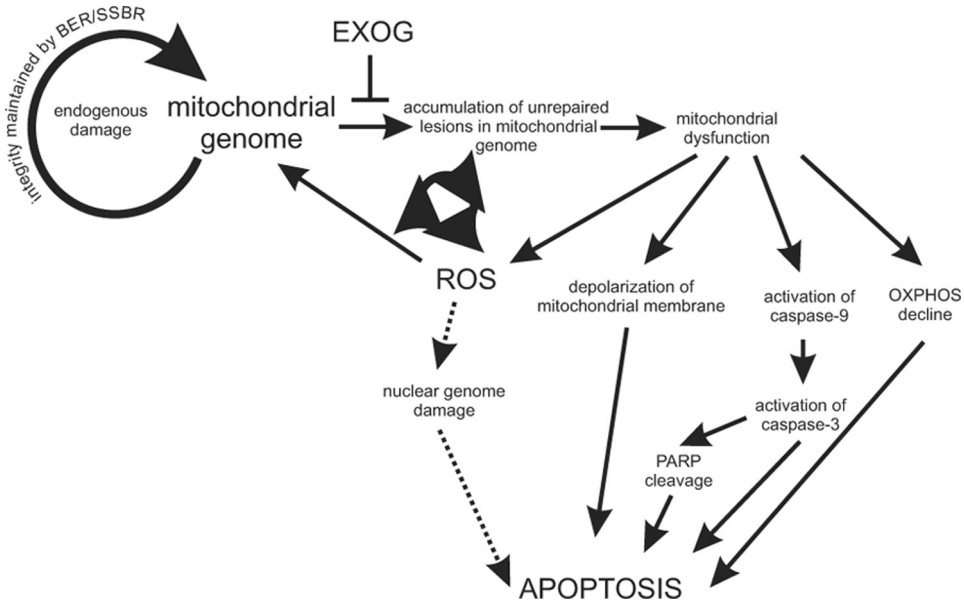

FIGURE 6. **Model for cell death triggered by accumulation of SSBs in the mt genome.**

peptide in both parental and rho0 cell lines (Fig. 5*B*). Although EXOG depletion caused 3- and 4-fold increase in early and late apoptotic cell populations in mtDNA containing normal A549 cells, there was no significant increase in the number of apoptotic cells in A549 rho0 cells compared with control siRNA-treated cells (Fig. 5, *C* and *D*). To confirm that apoptosis could be induced in A549 rho0 cells, we incubated these cells with 50 μM etoposide, a nuclear DNA topoisomerase II inhibitor (46), and observed a significant fraction of apoptotic cells (supplemental Fig. 8). In addition, depolarization of the mt membrane potential in A549 rho0 cells was not affected after EXOG depletion in contrast to that in A549 cells (Fig. 5*E*). These results together with those in Fig. 2 indicate that mt dysfunction due to EXOG depletion is directly linked to mt genome integrity and thus provide the first direct evidence that persistent SSBs specifically in the mt genome activate intrinsic apoptosis.

DISCUSSION

Our results show that EXOG is an essential component of the BER/SSBR in the mitochondria whose depletion causes accumulation of unrepaired SSBs specifically in the mt genome, triggering intrinsic apoptotic pathway. We propose that compromising the integrity of the mt genome causes mt dysfunction reflected by depolarization of mt membrane potential, OXPHOS decline, and a spiraling increase in ROS levels that further damage the mt genome as the immediate target, and subsequently the nu genome (Fig. 6). Here we have also shown that EXOG forms a complex with mt repair proteins, APE1, DNA pol γ, and DNA lig3, to carry out SSBR, and its activity could not be compensated by other mt 5′-exonucleases, in support of our previous results (18). We should point out that the timeline of cellular events due to EXOG depletion warrants detailed analysis because some of these events could occur simultaneously.

EXOG was identified as a dimeric mitochondrion-specific enzyme, with a *bona fide* mitochondrial leader sequence, which in contrast to EndoG possesses 5′-exonuclease activity (22, 30). Moreover, although mammalian EndoG acts on single- or double-stranded DNA and RNA at similar rates, EXOG was found to prefer single-stranded DNA substrate (22). Such a difference in substrate specificity suggests distinct cellular functions of EXOG and EndoG. EndoG plays a role in cell proliferation and DNA recombination (47) in addition to its well established function in cell death (32). Our results suggest a critical role of EXOG in maintaining mt genome integrity as a component of the mt BER/SSBR machinery. The roles of two other two 5′-exo/endonucleases, DNA2 and FEN1, for mt genome repair appear to be more complex. Yeast DNA2 (yDNA2), with 5′–3′-DNA-dependent helicase and ATPase activity on forked DNA, together with exonuclease activity with protruding ssDNA, was identified as an essential nuclear protein (48, 49). Both DNA2 and FEN1 were proposed to be involved in maturation of Okazaki fragments during DNA replication in yeast (50). The recombinant human DNA2 (hDNA2) shows similar enzymatic activity as yDNA2 (51) and interacts with FEN1 suggesting their complementary role during nDNA replication (52). Interestingly, in contrast to the situation in yeast, hDNA2 was initially proposed to be localized exclusively in the mitochondria (21), although its nuclear localization was subsequently established (53). Depletion of hDNA2 reduced the level of mtDNA replication intermediate (53). Interaction of hDNA2 with DNA pol γ, the only DNA polymerase in mitochondria involved in both replication and repair, further supports its important role in biogenesis of mt genome (21). It was suggested that hDNA2 together with FEN1 processes flap intermediates during mtDNA replication and repair (19).

Mouse and human cells depleted of individual DNA glycosylases do not show strong cellular effect/phenotype despite significant accumulation of multiple oxidatively damaged bases (54–57). It thus appears that extensive accumulation of oxidative DNA base lesions, in nu and mt genomes, does not limit life span of mice nor cause severe cellular effects (58, 59). Con-

versely, cells depleted from mtDNA pol γ, DNA lig3, FEN1, or APE1 are embryonic lethal in mouse or cause apoptosis in cultured cells (60–63). Thus, maintaining integrity of mt and nu genomes via faithful SSBR is a prerequisite for cell survival. Here, we have shown that EXOG is critical for integrity of mt genome, and its depletion triggers the intrinsic apoptotic pathway. More importantly, this trigger is absent in cells deficient in mtDNA. Although the rho0 cells do not exist naturally, they provide a unique opportunity for studying the role of mtDNA in cellular processes (64–66). However, how mt damage triggers cellular signaling to activate the cellular apoptosis warrants further investigation. In response to nDNA damage, eukaryotic cells activate a kinase-based checkpoint signaling network to arrest cell cycle progression and recruit repair machinery or trigger programmed cell death or senescence if the damage is extensive (67–69). The DNA damage-response network can be divided into two major protein kinase signaling branches that function through the upstream kinases, ataxia telangiectasia-mutated (ATM) and ATM and Rad3-related (ATR), which are critical initiators of the G_1/S, intra-S, and G_2/M cell cycle checkpoints through activation of their downstream effector kinases Chk2 and Chk1, respectively (69–72). Phosphorylation of Chk2 was recently shown to be significantly enhanced in cells with mtDNA damage caused by menadione treatment leading to G_2-M cell cycle arrest (73).

In conclusion, we have provided the first evidence that mt genome damage alone activates programmed cell death. Furthermore, depletion of EXOG could unravel the signaling pathways activated by mtDNA damage. EXOG could be explored as a therapeutic target to initiate tumor cell death.

Acknowledgments—We thank Drs. Sarah Toombs-Smith and David Konkel for critically editing the manuscript.

REFERENCES

1. Robin, E. D., and Wong, R. (1988) *J. Cell. Physiol.* **136,** 507–513
2. Miller, F. J., Rosenfeldt, F. L., Zhang, C., Linnane, A. W., and Nagley, P. (2003) *Nucleic Acids Res.* **31,** e61
3. Anderson, S., Bankier, A. T., Barrell, B. G., de Bruijn, M. H., Coulson, A. R., Drouin, J., Eperon, I. C., Nierlich, D. P., Roe, B. A., Sanger, F., Schreier, P. H., Smith, A. J., Staden, R., and Young, I. G. (1981) *Nature* **290,** 457–465
4. Turrens, J. F. (2003) *J. Physiol.* **552,** 335–344
5. Staniek, K., and Nohl, H. (2000) *Biochim. Biophys. Acta* **1460,** 268–275
6. St-Pierre, J., Buckingham, J. A., Roebuck, S. J., and Brand, M. D. (2002) *J. Biol. Chem.* **277,** 44784–44790
7. Cadenas, E., and Davies, K. J. (2000) *Free Radic. Biol. Med.* **29,** 222–230
8. Wallace, S. S. (2002) *Free Radic. Biol. Med.* **33,** 1–14
9. Caldecott, K. W. (2008) *Nat. Rev. Genet.* **9,** 619–631
10. Pesole, G., Gissi, C., De Chirico, A., and Saccone, C. (1999) *J. Mol. Evol.* **48,** 427–434
11. Almeida, K. H., and Sobol, R. W. (2007) *DNA Repair* **6,** 695–711
12. Fortini, P., and Dogliotti, E. (2007) *DNA Repair* **6,** 398–409
13. Hegde, M. L., Hazra, T. K., and Mitra, S. (2008) *Cell Res.* **18,** 27–47
14. Longley, M. J., Prasad, R., Srivastava, D. K., Wilson, S. H., and Copeland, W. C. (1998) *Proc. Natl. Acad. Sci. U.S.A.* **95,** 12244–12248
15. Liu, Y., Kao, H. I., and Bambara, R. A. (2004) *Annu. Rev. Biochem.* **73,** 589–615
16. Pinz, K. G., and Bogenhagen, D. F. (1998) *Mol. Cell. Biol.* **18,** 1257–1265
17. Stierum, R. H., Dianov, G. L., and Bohr, V. A. (1999) *Nucleic Acids Res.* **27,** 3712–3719
18. Szczesny, B., Tann, A. W., Longley, M. J., Copeland, W. C., and Mitra, S. (2008) *J. Biol. Chem.* **283,** 26349–26356
19. Liu, P., Qian, L., Sung, J. S., de Souza-Pinto, N. C., Zheng, L., Bogenhagen, D. F., Bohr, V. A., Wilson, D. M., 3rd, Shen, B., and Demple, B. (2008) *Mol. Cell. Biol.* **28,** 4975–4987
20. Akbari, M., Visnes, T., Krokan, H. E., and Otterlei, M. (2008) *DNA Repair* **7,** 605–616
21. Zheng, L., Zhou, M., Guo, Z., Lu, H., Qian, L., Dai, H., Qiu, J., Yakubovskaya, E., Bogenhagen, D. F., Demple, B., and Shen, B. (2008) *Mol. Cell* **32,** 325–336
22. Cymerman, I. A., Chung, I., Beckmann, B. M., Bujnicki, J. M., and Meiss, G. (2008) *Nucleic Acids Res.* **36,** 1369–1379
23. Marchetti, P., Susin, S. A., Decaudin, D., Gamen, S., Castedo, M., Hirsch, T., Zamzami, N., Naval, J., Senik, A., and Kroemer, G. (1996) *Cancer Res.* **56,** 2033–2038
24. Szczesny, B., Tann, A. W., and Mitra, S. (2010) *Mech. Ageing Dev.* **131,** 330–337
25. Ramana, C. V., Boldogh, I., Izumi, T., and Mitra, S. (1998) *Proc. Natl. Acad. Sci. U.S.A.* **95,** 5061–5066
26. Qian, W., and Van Houten, B. (2010) *Methods* **51,** 452–457
27. Santos, J. H., Meyer, J. N., Mandavilli, B. S., and Van Houten, B. (2006) *Methods Mol. Biol.* **314,** 183–199
28. Das, A., Wiederhold, L., Leppard, J. B., Kedar, P., Prasad, R., Wang, H., Boldogh, I., Karimi-Busheri, F., Weinfeld, M., Tomkinson, A. E., Wilson, S. H., Mitra, S., and Hazra, T. K. (2006) *DNA Repair* **5,** 1439–1448
29. Izumi, T., and Mitra, S. (1998) *Carcinogenesis* **19,** 525–527
30. Kieper, J., Lauber, C., Gimadutdinow, O., Urbańska, A., Cymerman, I., Ghosh, M., Szczesny, B., and Meiss, G. (2010) *Protein Exp. Purif.* **73,** 99–106
31. Patel, V. A., Longacre, A., Hsiao, K., Fan, H., Meng, F., Mitchell, J. E., Rauch, J., Ucker, D. S., and Levine, J. S. (2006) *J. Biol. Chem.* **281,** 4663–4670
32. Büttner, S., Eisenberg, T., Carmona-Gutierrez, D., Ruli, D., Knauer, H., Ruckenstuhl, C., Sigrist, C., Wissing, S., Kollroser, M., Fröhlich, K. U., Sigrist, S., and Madeo, F. (2007) *Mol. Cell* **25,** 233–246
33. Falkenberg, M., Larsson, N. G., and Gustafsson, C. M. (2007) *Annu. Rev. Biochem.* **76,** 679–699
34. Lizard, G., Miguet, C., Gueldry, S., Monier, S., and Gambert, P. (1997) *Ann. Pathol.* **17,** 61–66
35. Taylor, R. C., Cullen, S. P., and Martin, S. J. (2008) *Nat. Rev. Mol. Cell Biol.* **9,** 231–241
36. Tait, S. W., and Green, D. R. (2010) *Nat. Rev. Mol. Cell Biol.* **11,** 621–632
37. Bratton, S. B., Walker, G., Srinivasula, S. M., Sun, X. M., Butterworth, M., Alnemri, E. S., and Cohen, G. M. (2001) *EMBO J.* **20,** 998–1009
38. Nicholson, D. W., Ali, A., Thornberry, N. A., Vaillancourt, J. P., Ding, C. K., Gallant, M., Gareau, Y., Griffin, P. R., Labelle, M., and Lazebnik, Y. A., *et al.* (1995) *Nature* **376,** 37–43
39. Boulares, A. H., Yakovlev, A. G., Ivanova, V., Stoica, B. A., Wang, G., Iyer, S., and Smulson, M. (1999) *J. Biol. Chem.* **274,** 22932–22940
40. Kroemer, G., Zamzami, N., and Susin, S. A. (1997) *Immunol. Today* **18,** 44–51
41. Yang, X. H., Sladek, T. L., Liu, X., Butler, B. R., Froelich, C. J., and Thor, A. D. (2001) *Cancer Res.* **61,** 348–354
42. Yang, X. H., Edgerton, S., and Thor, A. D. (2005) *Int. J. Oncol.* **26,** 1675–1680
43. Meyer, J. N. (2010) *Ecotoxicology* **19,** 804–811
44. Singh, N. P., McCoy, M. T., Tice, R. R., and Schneider, E. L. (1988) *Exp. Cell Res.* **175,** 184–191
45. Shen, B., Singh, P., Liu, R., Qiu, J., Zheng, L., Finger, L. D., and Alas, S. (2005) *BioEssays* **27,** 717–729
46. Panduri, V., Weitzman, S. A., Chandel, N. S., and Kamp, D. W. (2004) *Am. J. Physiol. Lung Cell. Mol. Physiol.* **286,** L1220–L1227
47. Huang, K. J., Ku, C. C., and Lehman, I. R. (2006) *Proc. Natl. Acad. Sci. U.S.A.* **103,** 8995–9000
48. Budd, M. E., and Campbell, J. L. (1995) *Proc. Natl. Acad. Sci. U.S.A.* **92,** 7642–7646
49. Bae, S. H., and Seo, Y. S. (2000) *J. Biol. Chem.* **275,** 38022–38031
50. Budd, M. E., and Campbell, J. L. (1997) *Mol. Cell. Biol.* **17,** 2136–2142
51. Masuda-Sasa, T., Imamura, O., and Campbell, J. L. (2006) *Nucleic Acids*

Res. **34,** 1865–1875
52. Kim, J. H., Kim, H. D., Ryu, G. H., Kim, D. H., Hurwitz, J., and Seo, Y. S. (2006) *Nucleic Acids Res.* **34,** 1854–1864
53. Duxin, J. P., Dao, B., Martinsson, P., Rajala, N., Guittat, L., Campbell, J. L., Spelbrink, J. N., and Stewart, S. A. (2009) *Mol. Cell. Biol.* **29,** 4274–4282
54. Arai, T., Kelly, V. P., Minowa, O., Noda, T., and Nishimura, S. (2006) *Toxicology* **221,** 179–186
55. Nilsen, H., Rosewell, I., Robins, P., Skjelbred, C. F., Andersen, S., Slupphaug, G., Daly, G., Krokan, H. E., Lindahl, T., and Barnes, D. E. (2000) *Mol. Cell* **5,** 1059–1065
56. Takao, M., Kanno, S., Shiromoto, T., Hasegawa, R., Ide, H., Ikeda, S., Sarker, A. H., Seki, S., Xing, J. Z., Le, X. C., Weinfeld, M., Kobayashi, K., Miyazaki, J., Muijtjens, M., Hoeijmakers, J. H., van der Horst, G., Yasui, A., and Sarker, A. H. (2002) *EMBO J.* **21,** 3486–3493
57. Vartanian, V., Lowell, B., Minko, I. G., Wood, T. G., Ceci, J. D., George, S., Ballinger, S. W., Corless, C. L., McCullough, A. K., and Lloyd, R. S. (2006) *Proc. Natl. Acad. Sci. U.S.A.* **103,** 1864–1869
58. Jang, Y. C., and Remmen, V. H. (2009) *Exp. Gerontol.* **44,** 256–260
59. Pérez, V. I., Bokov, A., Van Remmen, H., Mele, J., Ran, Q., Ikeno, Y., and Richardson, A. (2009) *Biochim. Biophys. Acta* **1790,** 1005–1014
60. Hance, N., Ekstrand, M. I., and Trifunovic, A. (2005) *Hum. Mol. Genet.* **14,** 1775–1783
61. Puebla-Osorio, N., Lacey, D. B., Alt, F. W., and Zhu, C. (2006) *Mol. Cell. Biol.* **26,** 3935–3941
62. Kucherlapati, M., Yang, K., Kuraguchi, M., Zhao, J., Lia, M., Heyer, J., Kane, M. F., Fan, K., Russell, R., Brown, A. M., Kneitz, B., Edelmann, W., Kolodner, R. D., Lipkin, M., and Kucherlapati, R. (2002) *Proc. Natl. Acad. Sci. U.S.A.* **99,** 9924–9929
63. Izumi, T., Brown, D. B., Naidu, C. V., Bhakat, K. K., Macinnes, M. A., Saito, H., Chen, D. J., and Mitra, S. (2005) *Proc. Natl. Acad. Sci. U.S.A.* **102,** 5739–5743
64. Appleby, R. D., Porteous, W. K., Hughes, G., James, A. M., Shannon, D., Wei, Y. H., and Murphy, M. P. (1999) *Eur. J. Biochem.* **262,** 108–116
65. Buchet, K., and Godinot, C. (1998) *J. Biol. Chem.* **273,** 22983–22989
66. Stuart, J. A., Hashiguchi, K., Wilson, D. M., 3rd, Copeland, W. C., Souza-Pinto, N. C., and Bohr, V. A. (2004) *Nucleic Acids Res.* **32,** 2181–2192
67. Abraham, R. T. (2001) *Genes Dev.* **15,** 2177–2196
68. Harper, J. W., and Elledge, S. J. (2007) *Mol. Cell* **28,** 739–745
69. Jackson, S. P., and Bartek, J. (2009) *Nature* **461,** 1071–1078
70. Bartek, J., and Lukas, J. (2003) *Cancer Cell* **3,** 421–429
71. Kastan, M. B., and Bartek, J. (2004) *Nature* **432,** 316–323
72. Shiloh, Y. (2003) *Nat. Rev. Cancer* **3,** 155–168
73. Koczor, C. A., Shokolenko, I. N., Boyd, A. K., Balk, S. P., Wilson, G. L., and Ledoux, S. P. (2009) *J. Biol. Chem.* **284,** 36191–36201